Effect of Gravity Model Inaccuracy on Navigation Performance

A. B. Chatfield,* M. M. Bennett,† and T. Chen‡
Geodynamics Corporation, Santa Barbara, Calif.

Instead of the usual treatment of gravity model errors in terms of uncertainties with assumed statistical characteristics, the navigation errors for a selected flight path were derived from simulations of the navigation process with an accurate reference gravity model and with an ellipsoid model. The deterministic error due to use of the ellipsoid gravity model in the navigation computations was obtained for the selected flight path by differencing the navigation state obtained with the two gravity models. The reference gravity model is composed of the $C_{0,0}$ and $C_{2,0}$ spherical harmonic coefficients and a large number of subterranean point masses. The point mass values were determined by least-squares fitting to mean gravity disturbances derived from surface mean gravity anomalies and associated geoid heights. Uncertainties in these data were used to establish the uncertainty in the evaluation of the deterministic navigation error for the selected flight path.

Introduction

NAVIGATION system operations may be divided int two broad categories—single trips over a large number of vehicle trajectories within a region of specific boundaries and repeated operation along a single route. The statistical effect of gravity model inaccuracy on navigation system performance is distinctly different for these two types of operation because of the variability of the gravity field with geographic location.

In the first type of operation, the navigation error due to use of an ellipsoid gravity model would be expected to exhibit a mean and standard error as a function of navigation time. An accurate evaluation of the ensemble mean and ensemble standard error would involve repeated evaluations of the navigation error due to gravity model errors within the specified operational region.

A number of trips along a single route (such as during a navigation test program) result in the vehicle repeatedly passing through very nearly the same gravity field. As a consequence, the navigation errors due to use of an ellipsoid gravity model are algebraic functions of time, just as they are for a single trip.

With only a limited number of exceptions, such as the work reported in Ref. 1, the navigation uncertainty due to gravity model uncertainty has been determined to date without noting any distinction between types of operations.[2-5] In Ref. 1 specific statistical treatment of complex vehicle paths is considered.

More importantly, available gravity field data have not been fully utilized to reduce navigation inaccuracy due to gravity model inaccuracy.[1-5] In those cases in which attempts have been made to use available gravity data, the navigation system employed partial compensation by including the gravity model error in the state vector being estimated.[3,4] Information on the measured gravity field was incorporated into the navigation computations in the form of Markov models.

Until a method of deriving an accurate reference gravity model became available there was no attractive alternative to these navigation error analysis approaches except the use of interpolation between stored values of the gravity anomaly and deflections of the vertical. This procedure is accurate and practical for ground navigation in a relatively small geographic area. However, the awesome task of extrapolating deflections of the vertical to the flight altitude over a large area and the possible requirement to generate extrapolated values for several altitudes make this method unattractive even for postflight analysis.

With the advent of a method of deriving a reference gravity model which accurately reproduces the gravity field in a deep volume of space over a large geographic area, it is now possible by direct simulation to establish accurately and conveniently the deterministic gravity model error and remove its effect from both inertial and aided-inertial navigation, thereby greatly reducing the navigation uncertainty in regions where the gravity field is well mapped.

This paper presents the results of an evaluation of the effect of gravity model inaccuracy on an aircraft navigation system operating in both inertial and aided-inertial modes. The error analyses are based upon one north-south round trip flight between Southern New Mexico and Northern Colorado. Flight altitude, speed, and navigation time were 20,000 ft, 380 knots, and 2 hr and 49 min., respectively. Navigation state for the inertial navigation simulations included velocity, position, and attitude. The state vector used in the aided-inertial navigation simulation included, in addition, the gravity model error. Doppler velocity measurements were utilized at 3-min intervals except during turns, and checkpoint geodetic coordinate updates were utilized at intervals of approximately 10 min.

The results of the error analysis show the effect of gravity model inaccuracy for a flight test type of operation over the selected flight path. Obtaining the ensemble mean and standard error for a large operational region will require extension of the reference gravity model to a larger geographic area and repeated application of the error analysis procedure described here.

Basic Definitions

The reference gravity model is defined as the set of ellipsoid spherical harmonic coefficients and point masses which best fits, in a least-squares sense, a set of gravity disturbance vectors generated from mean free-air gravity anomalies and associated geoid heights.§ Thus, in a least-squares sense, it is a

Received October 22, 1974; revision received February 27, 1975. This research was supported by the Missile Guidance and Technology Branch, Guidance Division, Space & Missile Systems Command, Air Force Systems Command.

Index category: Navigation, Control, and Guidance Theory.

*Manager, Theory and Analysis Department.

†President.

‡Member of Technical Staff. Member AIAA.

§Terms common to geodesy but not frequently encountered in the aerospace industry, such as gravity anomaly and geoid height, are defined in Ref. 3.

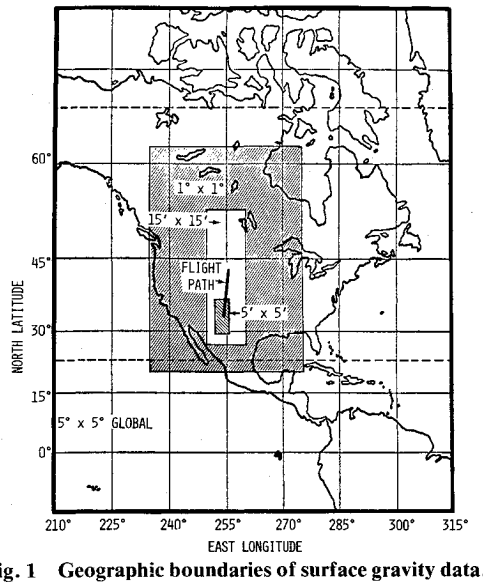

Fig. 1 Geographic boundaries of surface gravity data.

best-estimate gravity model and functionally dependent parameters are symbolically indicated by the subscript B. The ellipsoid gravity model is referred to as the simplified model and functionally dependent parameters are denoted by the subscript S.

For a given vehicle path, the error in navigation state due to use of gravity derived from a simplified model is an algebraic function of time. Denoting this algebraic function of time by $\Delta\tilde{X}_G(t)$, the defining relation is

$$\Delta\tilde{X}_G(t) \triangleq \tilde{X}_S(t) - X_A(t) \tag{1}$$

where $X_A(t)$ = error-free state associated with the vehicle trajectory generated with the actual (true) gravity field and a reference specific force profile, $\tilde{X}_S(t)$ = error-free navigation system estimate of state based on use of the simplified gravity model and the reference specific force profile.

The error-free navigation state generated with the reference gravity model and the reference specific force profile $X_B(t)$ may be subtracted and added to the right side of Eq. (1) to yield

$$\Delta\tilde{X}_G(t) = \Delta\tilde{X}_{GS}(t) + \Delta X_{GD}(t) \tag{2}$$

in which

$$\Delta\tilde{X}_{GS}(t) \triangleq \tilde{X}_S(t) - X_B(t) \tag{3}$$

$$\Delta X_{GD}(t) \triangleq X_B(t) - X_A(t) \tag{4}$$

The $\Delta\tilde{X}_{GS}(t)$ term in Eq. (2) represents that portion of the systematic error in navigation state due to unmodeled gravity errors which is deterministic and can be evaluated by simulating navigation computations using the reference gravity model and the simplified gravity model. The remaining term $\Delta X_{GD}(t)$ represents the error in establishing $\Delta\tilde{X}_G(t)$ by use of the approximation $\Delta\tilde{X}_{GS}(t)$. It can only be evaluated on a statistical basis. The gravity-related causes for the existence of $\Delta X_{GD}(t)$ are threefold: 1) errors in the surface gravity data used in the generation of the reference gravity model, 2) geographic area and wavelength content limitations in the gravity data base, and 3) reduction of the reference gravity model residuals to small values but not to zero in the least-squares point mass function-fitting process. Sources 2 and 3 can be made negligibly small where sufficient surface gravity data are available and convergence of the modeling process is rigidly constrained. Since these two conditions are met for the selected flight-path region, the uncertainty in establishing $\Delta\tilde{X}_G(t)$ is due primarily to uncertainty in the surface gravity data.

A relatively straightforward method of evaluating the effect of gravity model data uncertainties is to employ an ensemble of navigation simulations based on perturbed reference gravity models. The perturbed reference gravity models are derived by a Monte Carlo process which involves randomly selecting perturbations in the gravity data based on gravity data uncertainty statistics. Denoting the error in navigation state corresponding to the ith perturbation of the reference gravity model by $\Delta\tilde{X}_{GD_i}(t)$, the defining relation is

$$\Delta\tilde{X}_{GD_i}(t) \triangleq \tilde{X}_{B_i}(t) - X_B(t) \tag{5}$$

where $\tilde{X}_{B_i}(t)$ = error-free navigation system estimate of state based on use of the ith perturbed reference gravity model and the reference specific force profile.

The description, given later, of the manner in which $\Delta\tilde{X}_{GS}(t)$ and the Cov $[\Delta\tilde{X}_{GD}(t)]$ are evaluated will be more readily understood if we first say a few words about the generation of the reference gravity model and the reference specific force profile.

Reference Gravity Model Generation

The reference gravity model used here is composed of the World Geodetic System 1966 (WGS66) $C_{0,0}$ and $C_{2,0}$ spherical harmonic coefficients and 10,722 subterranean point masses. Generation of this reference required surface gravity data and the software for converting these data into grids of subterranean point masses representing the actual gravity field over and above the adopted spherical harmonic model.

The surface gravity data requirements are determined by the region in which the model is to be employed and the minimum wavelength of the gravity field having significance. For navigation purposes, the slower and lower the navigated vehicle, the shorter the minimum wavelength that must be accommodated by the reference gravity model. This is due to the low natural frequency of inertial and aided-inertial navigation systems and the increase in frequency of gravity model error effects attendant with increasing ground speed and decreasing altitude.

The surface gravity data used to develop the reference gravity model were acquired from the gravity library maintained by the Defense Mapping Agency—Aerospace Center (DMAAC) in the form of mean free-air gravity anomalies and associated geoid heights for $5° \times 5°$ geographic quadrangles over the entire Earth and for $1° \times 1°$, $15' \times 15'$, and $5' \times 5'$ for portions of the North American continent.

It is desirable to minimize the number of point masses to reduce computing time while at the same time utilizing a sufficient number of point masses to insure an accurate representation of gravity along the vehicle path. Previous experience at selecting model data region boundaries for aircraft navigation purposes was nonexistent. However, a considerable body of experience exists for selecting model data regions for ballistic missile launch region and flight region gravity models. On the basis of this experience the boundaries of the surface gravity data for each quadrangle size were selected. These data are displayed in Fig. 1 for the $1° \times 1°$, $15' \times 15'$, and $5' \times 5'$ grid sizes. For comparison purposes, the North-South flight path selected for the analysis is shown in the figure.

A least-squares point mass function-fitting process is used to establish the mass ratios¶ of a set of subterranean point masses which will reproduce given surface gravity disturbances in a prescribed geographical area and which are capable of being used to evaluate disturbance gravity at altitude. The reference gravity model geographic boundaries, statistics of the mean disturbances, and the fitting residual statistics are listed in Tables 1 and 2. The residual statistics in Table 2 are shown at the beginning of the fitting process for each point mass subset after the contributions of previously fitted, more granular point mass subsets have been subracted

¶Ratio of the point mass to the mass of the earth.

Table 1 Surface gravity data limits and characteristics

Grid size	Geographic region limits: Upper lat (deg)	Lower lat (deg)	Left long (deg)	Right long (deg)	Mean disturbances (mgal)	RMS disturbances (mgal)	Minimum disturbances (mgal)	Maximum disturbances (mgal)	No. of mean disturbances
5°×5°	90.0	−90.0	0.0	360.0	.385	21.792	− 96.6	81.3	1662
1°×1°	62.0	20.0	235.0	275.0	15.979	23.187	− 92.7	101.7	1680
15′×15′	52.5	28.5	249.0	261.0	2.042	27.322	−209.1	84.1	4608
5′×5′	35.0	29.5	252.0	255.5	4.577	26.478	−131.5	78.0	2772
								Total	10722[a]

[a] Also number of point masses.

(0 iterations) and after the six to eight iterations required to get all residuals down to less than one mgal.

Reference Specific Force Profile Generation

The specific force profile is utilized to simulate the nominal thrust, lift, and drag accelerations experienced by the navigated vehicle and sensed by the navigation system accelerometers. The variation with navigation time is produced by a two-step procedure beginning with the generation of a total acceleration profile satisfying the end conditions of a series of segments (stages) which, end to end, make up the desired vehicle path. At selected integration time points, the gravity vector components are evaluated with the reference gravity model and subtracted from the total acceleration vector components to obtain the specific force vector components. End conditions for each stage are specified in terms of horizontal groundspeed, rhumb-line azimuth geodetic height, and the first and second time derivatives of these parameters. Variations during each stage were obtained from fifth-order polynomials with coefficients derived from the end conditions.

Because of the gravity feedback, gravity model errors cause divergence of the vertical channel, and most aircraft navigation systems employ an altimeter to control vertical position. The procedure described for deriving the reference specific force profile insures achievement of the desired geodetic height profile for the reference gravity model trajectory. To simulate navigation with an error-free pressure altimeter, the same height profile should be achieved when gravity is derived from the simplified gravity model or the perturbed reference gravity model. This requires a modification of the reference specific force profile, which was accomplished by adjusting the vertical component of the reference specific force profile by the amount required to cause the navigation trajectory to have the desired geodetic height profile.

Inertial Navigation Errors

For navigation systems employing no external measurements there is no estimated state $\tilde{X}_S(t)$ in the usual sense, but rather a calculated state $X_S(t)$, based on the simplified gravity model. The resulting navigation error at each time t is evaluated with Eq. (3) after replacing $\tilde{X}_S(t)$ by $X_S(t)$. Thus

$$\Delta\tilde{X}_{GS}(t) = X_S(t) - X_B(t) \tag{6}$$

in which

$$X_B(t) = X_B(t_0) + \begin{bmatrix} V_B(t) \\ P_B(t) \end{bmatrix} \tag{7}$$

$$X_S(t) = X_S(t_0) + \begin{bmatrix} V_S(t) \\ P_S(t) \end{bmatrix} \tag{8}$$

$$V_B(t) = \int_{t_0}^{t} [A(\tau) + g_B(P_B(\tau))]\,d\tau \tag{9}$$

Table 2 Point mass function-fitting statistics

Grid size	No. of iterations	Mean of residuals (mgals)	RMS of residuals (mgals)	Minimum residual (mgals)	Maximum residual (mgals)
5°×5°	0[a]	0.39	21.79	− 96.59	81.30
	8	−0.01	0.29	− 0.89	0.96
1°×1°	0[b]	1.04	16.49	− 81.74	87.77
	7	0.00	0.08	− 0.97	0.57
15′×15′	0[b]	−0.01	18.87	−152.21	84.58
	7	0.00	0.05	− 0.47	0.64
5′×5′	0[b]	−0.07	12.45	− 69.50	54.16
	6	0.00	0.05	− 0.45	0.70

[a] The data for the zero iteration applied before the fitting process was begun but after the contributions of the $C_{0,0}$ and $C_{2,0}$ spherical harmonic coefficients have been removed.

[b] The data for the zero iterations apply before the fitting process was begun but after the contribution of the more granular point mass subset has been removed.

$$V_S(t) = \int_{t_0}^{t} [A(\tau) + g_S(P_S(\tau))]\,d\tau \tag{10}$$

$$P_B(t) = \int_{t_0}^{t} V_B(\tau)\,d\tau \tag{11}$$

$$P_S(t) = \int_{t_0}^{t} V_S(\tau)\,d\tau \tag{12}$$

In these expressions $A(\tau)$ = reference specific force vector; $X_B(t_0)$, $X_S(t_0)$ = velocity and position vectors at the start of navigation (after completion of coarse and fine alignment, which are not part of the present study); $V_B(t)$, $V_S(t)$ = velocity vectors at time t; $P_B(t)$, $P_S(t)$ = position vectors at time t; $g_B(P_B(\tau))$, $g_S(P_S(\tau))$ = gravity vectors at time τ associated with positions derived with the reference and simplified gravity models, respectively; τ = dummy variable for time.

In the present study

$$X_B(t_0) = X_S(t_0) \tag{13}$$

because only gravity model attributable navigation errors are examined.

The results of the evaluation of the deterministic inertial navigation errors due to use of an ellipsoid gravity model in the navigation computations are displayed in Figs. 2-5. Figure 2 shows the gravity model error defined by

$$\Delta\tilde{g}_{GS}(t) = g_S(P_S(t)) - g_B(P_B(t)) \tag{14}$$

which is the driving force for the velocity, position, and attitude errors shown in Figs. 3, 4, and 5, respectively. The vertical component of the gravity model error is shown in Fig. 2, but was not a forcing function in the error analysis because of the clamping of the vertical channel.

The rough symmetry of the gravity model errors about the middle time point is, of course, due to the fact that the southbound leg of the flight nearly retraced the path followed during the northbound leg. The dimples in the velocity error curves in Fig. 3 are due to the rapid changes in the gravity

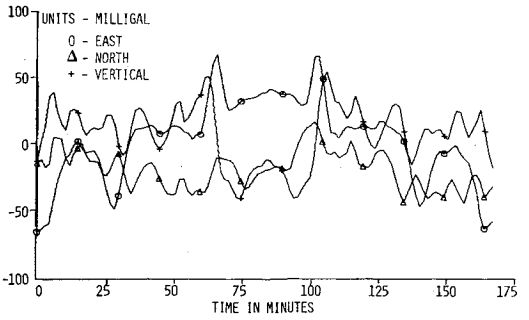

Fig. 2 Inertial navigation gravity model error for ellipsoid gravity model.

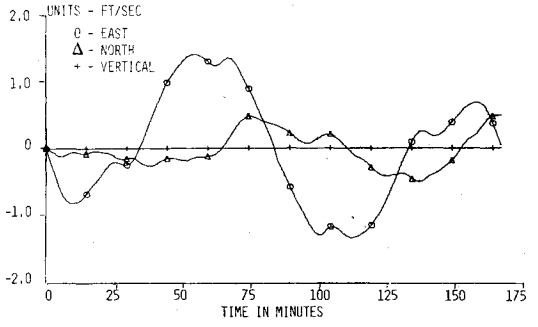

Fig. 3 Inertial navigation velocity error for ellipsoid gravity model.

model error during these times. The attitude errors in Fig. 5 are due solely to the east and north position errors, since there are no inertial equipment errors involved in the analysis.

Aided-Inertial Navigation Errors

An aided-inertial navigation system will periodically update the estimated state vector parameters on the basis of external measurements of velocity, position, or attitude. A filter gain matrix $K_{NF}(t)$ is evaluated and used to update the estimated state at time t, $\tilde{X}^{+}_{GS}(t)$, as follows

$$\tilde{X}^{+}_{GS}(t) = \tilde{X}^{-}_{GS}(t) + K_{NF}(t)\ \delta\tilde{Y}_{GS}(t) \tag{15}$$

in which $\delta\tilde{Y}_{GS}(t)$ is the measurement residual. Here and elsewhere the superscripts $-$ and $+$ denote the value of the estimated state vector just before and after the measurement update, respectively.

The subscript NF in Eq. (15) and subsequent expressions is meant to accentuate the fact that the parameter involved must derive from the same calculations employed in the actual navigation system filter. If available, the elements of $K_{NF}(t)$ would be the values generated in an actual navigation flight. Since such data are unlikely to be available, the gain matrix elements are evaluated using approximately the same vehicle trajectory and specific force profile, filter state vector parameter list, error models, initial state vector covariance, external measurement parameter list, and uncertainties as would be used in actual navigation computations. As a consequence, the results of the error analysis are valid only for the aided-inertial navigation configuration assumed. Different aided-inertial navigation configurations will have different deterministic navigation errors, even though the same flight path is employed.

The navigation system software is assumed to be based upon a Kalman-Bucy sequential filter.[6] Hence, the filter gain is given by

$$\begin{aligned} K_{NF}(t) &\triangleq E[\delta\tilde{X}^{-}_{NF}(t)\ \delta\tilde{Y}_{NF}(t)^T] \\ &\times \{E[\delta\tilde{Y}_{NF}(t)\delta\tilde{Y}_{NF}(t)^T]\}^{-1} \\ &= P^{-}_{X}(t)B(t)^T[B(t)P^{-}_{X}(t)B(t)^T \\ &+ P_Y(t_{-1})]^{-1} \end{aligned} \tag{16}$$

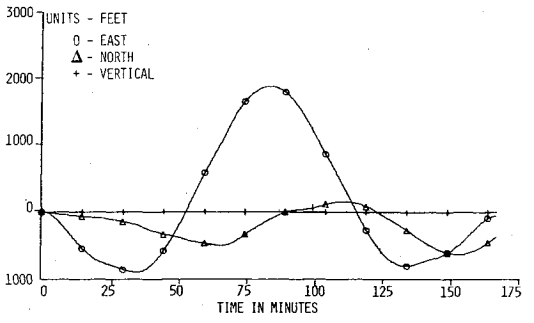

Fig. 4 Inertial navigation position error for ellipsoid gravity model.

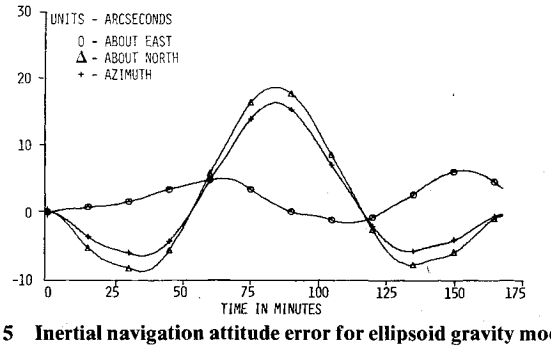

Fig. 5 Inertial navigation attitude error for ellipsoid gravity model.

where

$$\begin{aligned} P^{-}_{X}(t) &\triangleq E[\delta\tilde{X}^{-}_{NF}(t)\delta\tilde{X}^{-}_{NF}(t)^T] \\ &= [\phi_S(t,t_{-1})P^{+}_{X}(t_{-1}) \\ &+ \phi_{21}(t,t_{-1})]\phi_S(t,t_{-1})^T \end{aligned} \tag{17}$$

$$P^{+}_{X}(t) = [I - K_{NF}(t)B(t)]P^{-}_{X}(t)[I - K_{NF}(t)B(t)]^T + K_{NF}(t)P_Y(t)K_{NF}(t)^T \tag{18}$$

$$P_Y(t) \triangleq E[N_Y(t)N_Y(t)^T] \tag{19}$$

$$\phi_S(t,t_{-1}) = e^{\bar{F}_S\delta t} = \sum_{i=0}^{5} \frac{(\bar{F}_S\delta t)^i}{i!} \tag{20}**$$

$$\delta\tilde{Y}_{NF}(t) = B(t)\delta\tilde{X}^{-}_{NF}(t) + N_Y(t) \tag{21}$$

In these expressions $\delta\tilde{X}_{NF}(t)$ is the navigation filter state vector perturbation, $\delta\tilde{Y}_{NF}(t)$ the measurement residual, $\phi_S(t,t_{-1})$ the transition matrix across the integration step $\delta t = t - t_{-1} = 30$ sec, $N_Y(t)$ the measurement noise, and $\bar{F}_S$ the mean value of the system dynamics matrix. The $\phi_{21}(t,t_{-1})$ matrix in Eq. (17) was obtained in a manner described in the first part of Appendix B of Ref. 3.

In the derivation of the perturbation equations which define the system dynamics matrix F_S, no simplifications were introduced. The additional error analysis computation time due to including all terms is minor compared to that required for gravity evaluation.

In the aided-inertial mode the gravity model error is modeled as a first-order Markov process.[3-5] the gravity model error correlation distances and uncertainties at the beginning of navigation are typical of the values found in Refs. 3 and 5. The state vector characteristics are listed in Table 3.

The $B(t)$ matrix elements in the equations are the partial derivatives of the measurements with respect to the state vector parameters and are therefore a function of both. Defining relations for the measurements are provided following, along with appropriate values for the elements of the measurement covariance matrix $P_Y(t)$.

**Six terms were found to provide all the significant digits required.

Table 3 State vector characteristics

Parameter	Element no.	Initial standard error	Correlation distance
Velocity			
east, north	1, 2	1 knot	——
Position			
east, north	3, 4	300 ft	——
Attitude			
east, north	5, 6	18 sec	——
azimuth	7	180 sec	——
Gravity, model error			
east	8	24 mgal	30 n. mi.
north	9	24 mgal	15 n. mi.

Checkpoint Geodetic Coordinate Measurement

$$B(t) = \begin{bmatrix} \partial\phi^*/\partial\tilde{X}_{NF} \\ \partial\lambda/\partial\tilde{X}_{NF} \end{bmatrix}$$

$$= \begin{bmatrix} 0 & 0 & 0 & 1/(R_M+H) & 0 & 0 & 0 & 0 & 0 & 0 \\ 0 & 0 & \sec\phi^*/(R_N+H) & 0 & 0 & 0 & 0 & 0 & 0 & 0 \end{bmatrix} \quad (22)$$

$$R_N = a/(1-e^2\sin^2\phi^*)^{1/2} \quad (23)$$

$$R_M = a(1-e^2)/(1-e^2\sin^2\phi^*)^{3/2} \quad (24)$$

$$e = f(2-f) \quad (25)$$

$$P_Y(t) = \begin{bmatrix} \sigma_{\phi^*}^2 & 0 \\ 0 & \sigma_\lambda^2 \end{bmatrix} \quad (26)$$

where $\sigma_{\phi^*} = \sigma_\lambda = 3$ arc sec (random), H = geodetic height, ϕ^* = geodetic latitude, λ = geodetic longitude, a = semimajor axis of reference ellipsoid, f = reference ellipsoid flattening.

Doppler Radar Velocity Measurement††

$$B(t) = \begin{bmatrix} \partial V_H/\partial\tilde{X}_{NF} \\ \partial V_C/\partial\tilde{X}_{NF} \end{bmatrix}$$

$$= \begin{bmatrix} \sin\theta_H & \cos\theta_H & 0 & 0 & 0^{\ddagger\ddagger} & 0^{\ddagger\ddagger} & -(V_N\sin\theta_H - V_E\cos\theta_H) & 0 & 0 \\ \cos\theta_H & -\sin\theta_H & 0 & 0 & 0^{\ddagger\ddagger} & 0^{\ddagger\ddagger} & -(V_N\cos\theta_H + V_E\sin\theta_H) & 0 & 0 \end{bmatrix} \quad (27)$$

$$\theta_H = \tan^{-1}\left[\frac{V_E}{V_N}\right] \quad (28)$$

$$P_Y(t) = \begin{bmatrix} K_H V_g & 0 \\ 0 & K_C V_g \end{bmatrix} \quad (29)$$

$$V_g = (V_E^2 + V_N^2)^{1/2} \quad (30)$$

$$K_H = \pi\left(\frac{1852}{3600}\right)\left(\frac{P_H}{\delta t_d}\right) \quad (31)$$

$$K_C = \pi\left(\frac{1852}{3600}\right)\left(\frac{P_C}{\delta t_d}\right) \quad (32)$$

where $P_H = 4\times10^{-3}$ knots^2/(rad/sec)/knot; $P_C = 6\times10^{-3}$ knots^2/(rad/sec)/knot; $\delta t_d = 10$ sec, V_H, V_C = along-heading and cross-heading doppler velocity components, respectively; V_E, V_N = east and north components of the navigation ground speed, respectively.

††Reference 4 discusses doppler radar error models.
‡‡Zero because vertical velocity is zero.

Effect of Gravity Model Errors on Residuals

Since only gravity model effects are being determined, the residual $\delta\tilde{Y}_{GS}(t)$ in Eq. (15) is the deviation of the measurement derived from the state associated with the reference gravity model from a similar measurement determined by the navigation system (based on use of the simplified gravity model) at the time of the measurement. As a consequence, the residual in the measurement vector due to use of a simplified gravity model is given by

$$\delta\tilde{Y}_{GS}(t) = f[X_B(t)] - f[\tilde{X}_S(t)] \quad (33)$$

where $f[\ ]$ denotes a function of the variable inside the brackets. Equations for the right side of this expression are provided below for both types of external measurements employed in the aided-inertial mode. The equations are written for the state associated with the reference gravity model $X_B(t)$. Identical expressions may be obtained for $f[\tilde{X}_S(t)]$ and $f[\tilde{X}_{B_i}(t)]$ by substituting the appropriate values for the parameters involved.

Checkpoint Geodetic Coordinate Measurement

$$f_{\phi^*}[X_B(t)] = \tan^{-1}\{\left[(1+K+p_B^2)Z_B + KP_B(b[(1+K+P_B^2)]^{1/2} - r_{XY_B}\right]/r_{XY_B}(1+P_B^2)\} \quad (34)$$

$$f_\lambda[X_B(t)] = \cos^{-1}\left[\frac{X_B}{r_{XY_B}}\right] = \sin^{-1}\left[\frac{Y_B}{r_{XY_B}}\right] \quad (35)$$

$$P_B = [(1+K)Z_B - Kh_B\sin\phi_B^*]/r_{XY_B} \quad (36)$$

$$h_B = r_{XY_B}\cos\phi_B^* + Z_B\sin\phi_B^* - a(1-e^2\sin^2\phi_B^*) \quad (37)$$

$$r_{XY_B} = (X_B^2 + Y_B^2)^{1/2} \quad (38)$$

$$K = e^2/(1-e^2) \quad (39)$$

$$[X_B Y_B Z_B] = (P_B^e)^T \quad (40)$$

where b = reference ellipsoid semiminor axis.

In the last expression, X_B, Y_B, and Z_B are the earth-centered, earth-fixed coordinates of the position vector. Equations (34, 36, and 37) indicate an iterative calculation is involved. Fortunately, the iterative procedure converges rapidly.[7]

Doppler Radar Velocity Measurement

$$f_V[X_B(t)] = C_v^d[V_B^v(t)]V_B^v(t) \quad (41)$$

$$V_B^v(t) = C_i^v(P_B^i)\ [\dot{P}_B^i - \omega_{ie}^i x P_B^i] \quad (42)$$

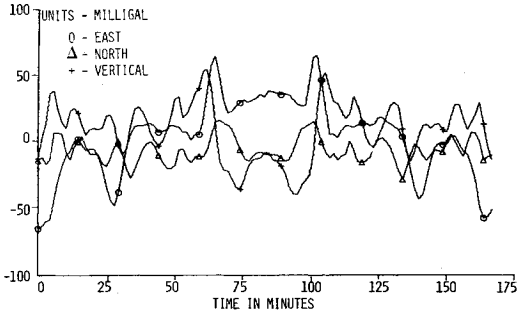

Fig. 6 Aided-inertial navigation gravity model error for ellipsoid gravity model.

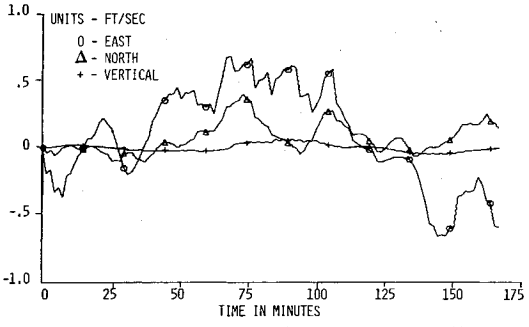

Fig. 7 Aided-inertial navigation velocity error for ellipsoid gravity model.

$$\begin{bmatrix} \dot{P}_B^{iT} & P_B^{iT} \end{bmatrix} = (X_B(t))^T \tag{43}$$

$$(\omega_{ie}^i)^T = [0 \;\; 0 \;\; \omega_{ie}] \tag{44}$$

where ω_{ie} = the earth's rotation rate.

The last equation is based on the assumption of zero pitch and roll angles, i.e., the doppler antenna is assumed to be stabilized to the local geodetic vertical. The parameters $\dot{P}_B^i$ and P_B^i denote velocity and position, respectively, in an earth-centered inertial coordinate system. Coordinate transformations between geodetic vertical and doppler antenna coordinates are denoted by $C_v^d[V_B^v(t)]$. The coordinate transformation between inertial and geodetic vertical coordinates $C_i^v(P_B^i)$ is defined by

$$C_v^d(V_B^v(t)) = \begin{bmatrix} \sin\theta_{H_B} & \cos\theta_{H_B} & 0 \\ \cos\theta_{H_B} & -\sin\theta_{H_B} & 0 \\ 0 & 0 & -1 \end{bmatrix} \tag{45}$$

$$C_i^v(P_B^i) = \begin{bmatrix} -\sin\lambda_{B_i} & \cos\lambda_{B_i} & 0 \\ -\sin\phi_B^*\cos\lambda_{B_i} & -\sin\phi_B^*\sin\lambda_{B_i} & \cos\phi_B^* \\ \cos\phi_B^*\cos\lambda_{B_i} & \cos\phi_B^*\sin\lambda_{B_i} & \sin\phi_B^* \end{bmatrix} \tag{46}$$

where

$$\lambda_{B_i} = \lambda_B + \omega_{ie}t \tag{47}$$

The gravity model error for aided-inertial navigation due to use of an ellipsoid gravity model is defined by

$$\Delta\tilde{g}_{GS}(t) = g_S[\tilde{P}_S(t)] - g_B[P_B(t)] \tag{48}$$

The east, north and vertical components of $\Delta\tilde{g}_{GS}(t)$ are plotted in Fig. 6 and the corresponding velocity, position, and attitude errors in Figs. 7-9, respectively. As in the plots for the inertial case, the vertical component of the gravity model error is shown, but was not a forcing function because of the clamping of the vertical channel. The slight departure from zero of the vertical components of the velocity and position errors in Figs. 7 and 8 are due to cross-coupling of horizontal errors into the vertical channel.

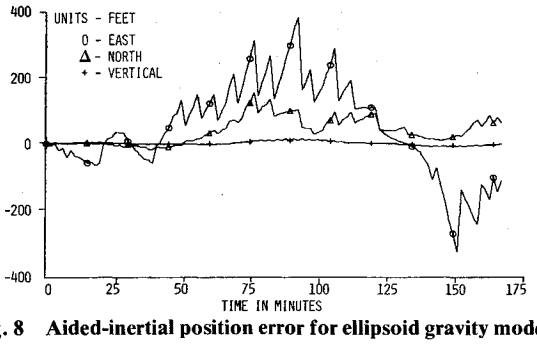

Fig. 8 Aided-inertial position error for ellipsoid gravity model.

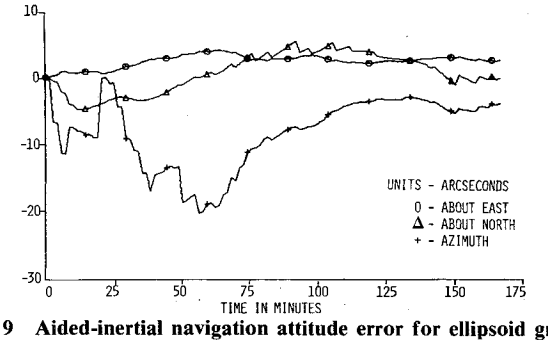

Fig. 9 Aided-inertial navigation attitude error for ellipsoid gravity model.

Table 4 Deterministic navigation error

Operational mode	Peak values Velocity (fps) east	north	position (ft) east	north
Inertial	+1.41	+.50	1883	165
	−1.34	−.50	−899	−622
12-State	+ .69	+.36	382	150
Aided-inertial	− .65	−.16	−327	− 20

Comparison of the velocity and position errors for the inertial and 12-state aided-inertial modes shows a marked change in the deterministic navigation error. Table 4 summarizes the change in terms of the peak positive and negative values of velocity and position errors. The results are apparently largely due to use of external measurements to estimate velocity, position, and attitude since the gravity model error for both modes is nearly identical. It appears that the first-order Markov model was not very effective. Assumption of a higher-order Markov process might bring about a small reduction in the navigation errors.

Generation of Perturbed Reference Gravity Models

An error in a mean anomaly derived from surface gravity measurements causes mean disturbance errors which, in turn, cause predictable errors in the nearby point mass ratios and, hence, in the value of gravity derived from the reference gravity model. Thus, the straightforward evaluation of the perturbations in gravity derived from the reference gravity model due to mean anomaly perturbations would involve the complex fitting process associated with the generation of the point mass ratios. The development of regression formulas relating disturbance vector perturbations directly to point mass ratio perturbations provides a convenient and accurate method of circumventing the fitting process. On physical grounds such as scheme appears possible because each point

Table 5 Regression coefficients for reference gravity model

Point mass set	a_1	a_2	a_3	a_4	a_5
$5° \times 5°$ [a]	−48.22	9.176	8.887	8.862	9.343
$1° \times 1°$ [b]	−16.68	1.972	4.064	4.108	1.969
$15' \times 15'$ [c]	−10.26	1.270	2.498	2.495	1.275
$5' \times 5'$ [d]	−12.03	1.658	2.624	2.631	1.644

[a] Coefficient values have been multiplied by 10^5.
[b] Coefficient values have been multiplied by 10^6.
[c] Coefficient values have been multiplied by 10^7.
[d] Coefficient values have been multiplied by 10^8.

mass ratio is primarily determined by the local mean disturbance vectors. A regression formula of the following type was found to be accurate to within less than 10% on the average

$$m(\phi^*,\lambda) = a_1\delta g(\phi^*,\lambda) + a_2\delta g(\phi^*+\Delta\phi^*,\lambda) + a_3\delta g(\phi^*,\lambda+\Delta\lambda) + a_4\delta g(\phi^*,\lambda-\Delta\lambda) + a_5\delta g(\phi^*-\Delta\phi^*,\lambda) \quad (49)$$

In this expression $m(\phi^*,\lambda)$ denotes a mass ratio which is a function of geodetic latitude and longitude and $\delta g(\phi^*,\lambda)$ denotes the geodetic vertical component of the disturbance vector, which is also a function of geodetic coordinates. The coefficients a_1 through a_5 are constants for each mean anomaly grid size. The $\Delta\phi^*$ and $\Delta\lambda$ increments correspond to this grid size. Thus, the perturbed value of the point mass ratio at the coordinates of the center of one of the grid sizes is determined by the perturbed value of the disturbance vector directly above and the perturbed values of the nearest disturbance vectors lying to the north, east, west, and south, respectively [see Eq. (49)]. The numerical solution coefficient values for each point mass set are listed in Table 5.

Uncertainty Due to Imperfections in Gravity Data

The uncertainty in establishing the deterministic error in navigation state due to the uncertainty in the mean gravity anomaly data§§ was assessed by repeated evaluations of Eq. (5) using the perturbed reference gravity models. By this means, perturbations in navigation state are obtained which are due to perturbations in the reference gravity derived from randomly selected perturbations in the mean anomaly data. Of course, the random perturbation selection was controlled so as to reproduce the data base uncertainty statistics for an ensemble of perturbations.

For operations involving single trips by the same navigated vehicle over many diverse trajectories within a specified operational region, the aforementioned navigation uncertainty can be established by repeating the analysis described in this section a number of times for a number of trajectories. For one trip, or for repeated trips along the same route, the navigation uncertainty will exhibit a specific variation with time, which will be different for each route

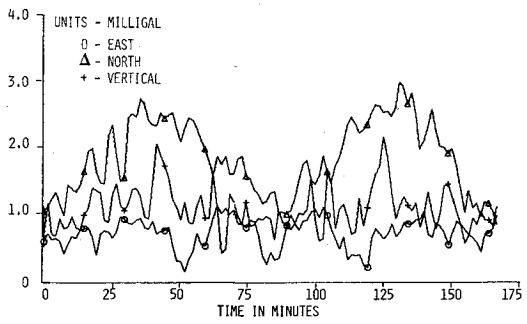

Fig. 10 Standard error in inertial navigation gravity.

§§2 mgal 1σ.

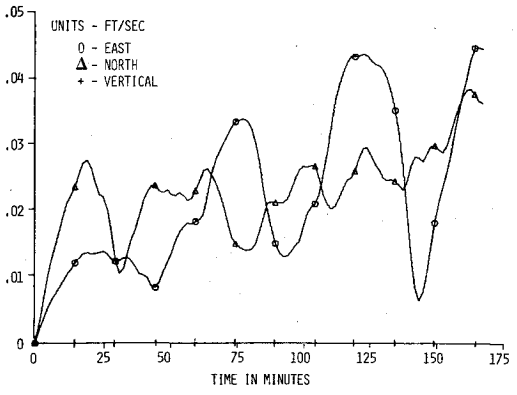

Fig. 11 Standard error in inertial navigation velocity.

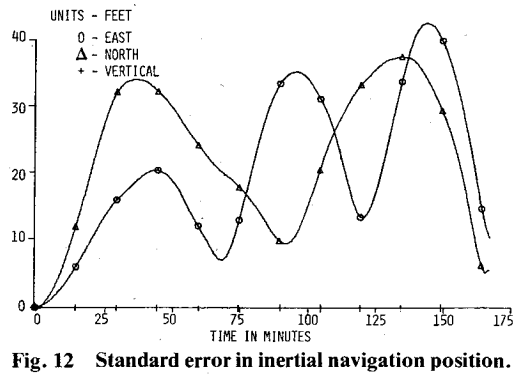

Fig. 12 Standard error in inertial navigation position.

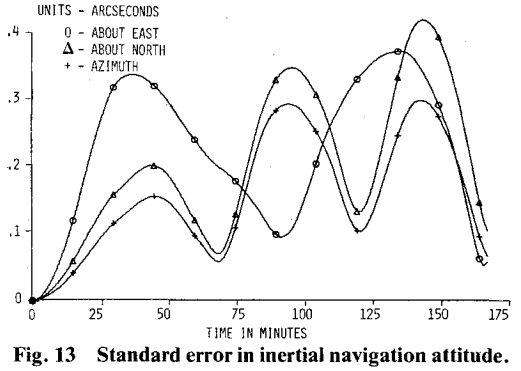

Fig. 13 Standard error in inertial navigation attitude.

because gravity data uncertainty varies with geographic location.

The uncertainty in establishing the deterministic error in the navigation state due to reference gravity model data uncertainties is described by the covariance of $\Delta\tilde{X}_{GD}(t)$, denoted Cov $[\Delta\tilde{X}_{GD}(t)]$, which is defined by the expected value of the product of $\Delta\tilde{X}_{GD}(t)$ and its transpose. In mathematical form

$$\text{Cov}[\Delta\tilde{X}_{GD}(t)] \triangleq E[\Delta\tilde{X}_{GD}(t)\Delta\tilde{X}_{GD}(t)^T] \quad (50)$$

where

$$\Delta\tilde{X}_{GD}(t) \triangleq [\Delta\tilde{X}_{GD_1}(t)\Delta\tilde{X}_{GD_2}(t)\ldots\Delta\tilde{X}_{GD_N}(t)] \quad (51)$$

Here, N is the number of times the reference gravity model data base is perturbed in the Monte Carlo process. As indicated by a comparison of Eqs. (3) and (5), the mathematical relations for evaluating $\Delta\tilde{X}_{GD_i}(t)$ are the equations provided with the S subscript replaced by B_i.

Based upon five perturbed reference gravity models, the uncertainty in the gravity model error shown in Fig. 2 is as provided in Fig. 10 for operation in the inertial mode. The corresponding uncertainties in the evaluations of the deterministic velocity, position, and attitude errors are displayed in Figs. 11-13, respectively. It is readily apparent from the

figures that the uncertainty in evaluating the deterministic navigation errors is very small, even if one makes allowances for the small number of reference gravity model perturbations employed in the error analysis. This result is, of course, due to the selection of a flight region in which the uncertainty ascribed to available mean free-air anomaly data is relatively low. In the aided-inertial mode the navigation standard errors are less than 0.03 fps for velocity, 12 ft for position, and 0.12 arc sec for attitude.

Conclusions

For the selected flight path, use of available gravity field data reduces inertial navigation velocity and position inaccuracy from peak values of 1.41 fps and 1883 ft to 0.05 fps and 40 ft, respectively. In the aided-inertial mode with doppler velocity and checkpoint position updates, the reduction is from 0.69 fps and 382 ft to 0.03 fps and 12 ft, respectively. This improvement in accuracy is achieved by evaluating the deterministic part of the navigation error using the method described in this paper (or any equivalent method) and removing the error from the navigation state as a function of time. The point mass model representation of the earth's complex gravity field provides a useful reference gravity model for evaluating the deterministic part of the navigation error.

The calculation of gravity using the reference model in real time would provide the same reduction in navigation state uncertainty mentioned previously, but it is probably not practical at present because of the computer storage and computation speed requirements associated with the evaluation of gravity from thousands of point masses.

The effect of gravity model inaccuracy is significantly reduced by use of external measurements processed through a Kalman filter. The reduction of 50% in velocity and 80% in position for the considered navigation configuration is primarily due to the inclusion of velocity, position, and attitude in the aided-inertial navigation state vector. Use of first-order Markov model for the gravity model uncertainty resulted in very little of the gravity model error being removed by the estimation process. Such a result is not surprising since there are two parameters involved in a first-order Markov model and 10,722 involved in the evaluation of the deterministic gravity model error. The development of more accurate models of the gravity model error is a subject for further investigation.

References

[1] Nash, R. A., Jr., "Effect of Vertical Deflections and Ocean Currents on a Maneuvering Ship," *IEEE Transactions on Aerospace and Electronics*, Vol. AES-4, Sept. 1968, pp. 329-338.

[2] Chovitz, R. H., "Statistical Analysis of the Effect of Deflection of the Vertical on Inertial Guidance Systems," written in collaboration with T. S. George, Air Force Missile Test Center, Rept. No. 16, June 1954, Army Map Service, Washington, D.C.

[3] Levine, S. A. and Gelb, A., "Effect of Deflections of the Vertical on the Performance of a Terrestrial Inertial Navigation System," *Journal of Spacecraft and Rockets*, Vol. 6, Sept. 1969, pp. 978-984.

[4] Nash, R. A. Jr., D'Appolito, J. A., and Roy, K. J., "Error Analysis of Hybrid Aircraft Inertial Navigation Systems," AIAA Paper 72-848, Stanford, Calif., 1972.

[5] Jordan, S. K., "Effect of Geodetic Uncertainties on a Damped Inertial Navigation System," *IEEE Transactions on Aerospace and Electronics*, Vol. AES-9, Sept. 1973, pp. 741-752.

[6] Bucy, R. S. and Joseph, P. D., "Applications of Filter Theory and Modeling Techniques," *Filtering for Stochastic Processes with Applications to Guidance*, Wiley, New York, 1968, pp. 140-141.

[7] Schreiter, J., "Space Rectangular Coordinates for Geodetic Positions with Elevations," Tech. Paper No. 71, Dec. 1949, Mapping & Charting Research Lab., Ohio State University, Columbus, Ohio.